Reduced Order Models for Dynamic Behavior of Elastomer Damping Devices

Benjamin Morin, Antoine Legay, Jean-François Deü

Reduced Order Models for Dynamic Behavior of Elastomer Damping Devices

Reduced Order Models for Dynamic Behavior of Elastomer Damping Devices

B. Morin, A. Legay and J.-F. Deü
LMSSC, Cnam, 292 rue Saint-Martin - 75141 Paris cedex 03
E-mail: benjamin.morin@cnam.fr

Abstract. In the context of passive damping, various mechanical systems from the space industry use elastomer components (shock absorbers, silent blocks, flexible joints...). The material of these devices has frequency, temperature and amplitude dependent characteristics. The associated numerical models, using viscoelastic and hyperelastic constitutive behaviour, may become computationally too expensive during a design process. The aim of this work is to propose efficient reduced viscoelastic models of rubber devices. The first step is to choose an accurate material model that represent the viscoelasticity. The second step is to reduce the rubber device finite element model to a super-element that keeps the frequency dependence. This reduced model is first built by taking into account the fact that the device's interfaces are much more rigid than the rubber core. To make use of this difference, kinematical constraints enforce the rigid body motion of these interfaces reducing the rubber device model to twelve dofs only on the interfaces (three rotations and three translations per face). Then, the super-element is built by using a component mode synthesis method. As an application, the dynamic behavior of a structure supported by four hourglass shaped rubber devices under harmonic loads is analysed to show the efficiency of the proposed approach.

1. Introduction

Due to their capacities to dissipate energy, elastomers are highly used in damping devices like silent blocs or joints. A typical example of this use is found in the spatial industry: during take off and flight, launchers are subject to a significant amount of vibrations from either the propulsion engine or the acoustical environment. Shocks may also occur during the pyrotechnic separation of the different floors of the launcher. All these vibration sources may damage the satellite or any other sensitive equipments on-board, and a common solution is to use viscoelastic damping devices to dissipate a part of the mechanical energy. The design and optimization of theses damping devices are usually done by using finite element codes. The computational cost of the associated models may become prohibitive. Many solutions already exist to reduce the numerical model of linear undamped structures, but only a few give access to reduced models with damping behavior, especially when it comes from viscoelasticity which may be seen as a strong form of damping. Two types of solutions for the reduction of viscoelastic models can be found in the literature. The first one is based on the theory of triboelasticity [6] and consists in the replacement of the damping device model by an equivalent rheological model which can be identified through a series of experimental measurements on the damper [7]. The main problem with this type of approach is that the behavior of the rheological model may not fit the real behavior of the damper in all directions, and more importantly it can't be used for

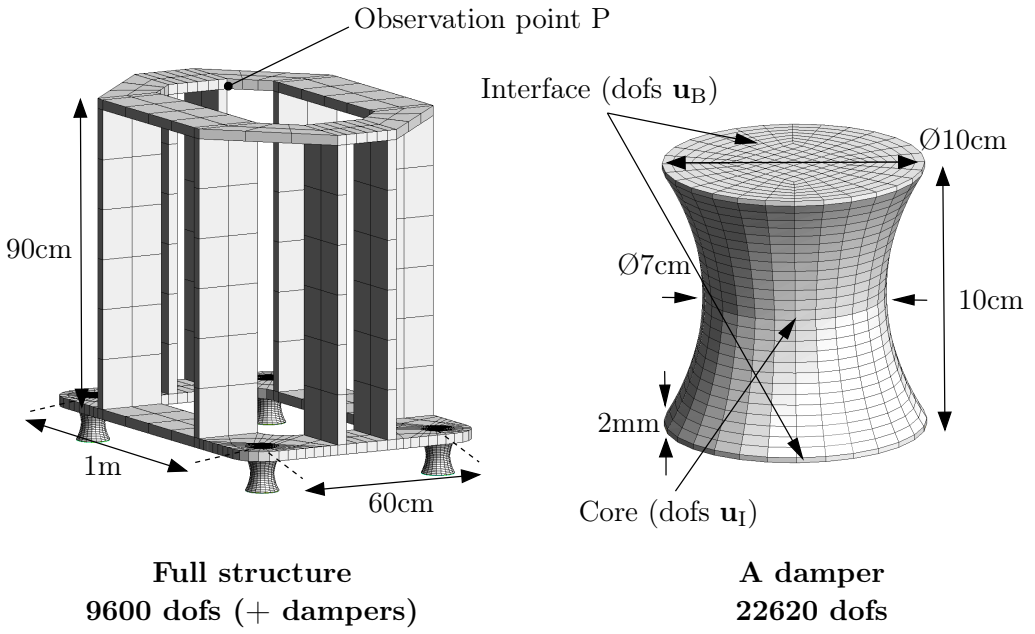

Figure 1. The complete structure mounted on four dampers, and details of a damper

a design purpose due to the non predictive aspect of the rheological model that is done for a specific geometry and material [8]. The second way of reducing a viscoelastic model is to extend the classical modal projection methods to the frequency dependent case and a review of the most common methods can be found in [2]. The chosen method in this work to achieve the reduction of the damper model is a modified Craig-Bampton method, based upon the work of Balmès [3] and Rouleau [2]. The original Craig-Bampton method [4] uses a combination of static and dynamic modes to reduce the finite element model of a sub-structure to a smaller finite element model called super-element. The super-element is first obtained by using a kinematical constraint to enforce rigid body motion of the sub-structure interfaces. Then, to further reduce the finite element model, the reduced finite element matrices are condensed onto the previously kinematically constrained interfaces. The combination of all these techniques leads to a twelve dofs super element replacing the initial full model.

2. Studied case and material models

The complete model is composed of a support structure mounted on four hourglass shaped dampers, as seen on figure (1). The support structure is made of aluminium and the dampers are made of two aluminium thin interface plates and an elastomer core. Two different material models are used: a classic linear elastic Hooke's model is chosen for the aluminium, and a viscoelastic fractional Zener model for the elastomer. This fractional model is defined by its complex frequency dependent modulus $\mathrm{G}^*(\omega)$:

$$\mathrm{G}^*(\omega) = \frac{\mathrm{G}_0 + \mathrm{G}_\infty(\mathrm{i}\omega\tau)^\alpha}{1 + (\mathrm{i}\omega\tau)^\alpha} \tag{1}$$

where G_0 and G_∞ are two asymptotic values: the static modulus $\mathrm{G}_0 = \mathrm{G}^*(\omega \to 0)$ and the high frequency limit of the dynamic modulus $\mathrm{G}_\infty = \mathrm{G}^*(\omega \to \infty)$. Also, τ is the relaxation time and α is the order of the fractional derivative. More information about this model, its identification and its finite element implementation in time domain can be found in [5]. The adimensional

viscoelastic modulus $\mathrm{G}^*(\omega)/\mathrm{G}_0$ is then used in the dynamic equation to take into account the viscoelastic behavior of the elastomer:

$$\left(\mathbf{K}^{\mathrm{e}} + \mathbf{K}^{\mathrm{v}}_{\mathrm{sph}} + \frac{\mathrm{G}^*(\omega)}{\mathrm{G}_0}\mathbf{K}^{\mathrm{v}}_{\mathrm{dev}} - \omega^2\mathbf{M}\right)\mathbf{u} = \mathbf{f} \tag{2}$$

where $\mathbf{M}$ is the mass matrix, $\mathbf{K}^{\mathrm{e}}$ is the purely elastic part of the stiffness matrix which is assembled on the aluminium interfaces dofs and $\mathbf{K}^{\mathrm{v}}$ is the viscoelastic part of the stiffness matrix which is assembled on the elastomer core dofs. The viscoleastic stiffness matrix is also separated into a spheric part $\mathbf{K}^{\mathrm{v}}_{\mathrm{sph}}$ and a deviatoric part $\mathbf{K}^{\mathrm{v}}_{\mathrm{dev}}$. This separation is used due to the fact that the viscoelastic behavior of elastomer is mainly caused by distorsional strain (not by volume change). This deviatoric stiffness matrix is the only matrix subjected to the complex modulus $G^*(\omega)$. The dynamic equation can also be expressed in terms of a static stiffness matrix $\mathbf{K}^0$ and a frequency dependent stiffness matrix $\mathbf{K}^\omega$:

$$\left(\mathbf{K}^0 + i\omega\mathrm{h}^*(\omega)\mathbf{K}^\omega - \omega^2\mathbf{M}\right)\mathbf{u} = \mathbf{f} \tag{3}$$

where $\mathbf{K}^0 = \mathbf{K}^{\mathrm{e}} + \mathbf{K}^{\mathrm{v}}_{\mathrm{sph}} + \mathbf{K}^{\mathrm{v}}_{\mathrm{dev}}$ and $\mathbf{K}^\omega = \left(\mathrm{G}_\infty/\mathrm{G}_0 - 1\right)\mathbf{K}^{\mathrm{v}}_{\mathrm{dev}}$. $\mathrm{h}^*(\omega)$ is a dimensionless frequency dependent modulus:

$$\mathrm{h}^*(\omega) = \frac{\tau^\alpha(i\omega)^{\alpha-1}}{1 + (i\omega\tau)^\alpha} \tag{4}$$

The material parameters used to build the mass and stiffness matrices are given in table 1 for the aluminium and table 2 for the elastomer. The materials parameters in table 2 comes from [1]. The structure is composed of 7540 nodes for each rubber damper, which is enough to get converged results in the frequency range of interest, and 3200 nodes for the upper aluminium structure. Only the computational cost of the dampers model is studied and reduced here, so the mesh of the upper structure is kept small for convenient computation time. Each damper represents 22620 dofs which are planed to be reduced to only 12 dofs with the proposed method. The total number of dofs in the complete structure is about 10^5, including more than 90% for the dampers only, thus underlining the need for an efficient reduction method. The finite element code for this study is an in house program developed in both Python and Fortran. The Python part is in charge for the global calculation of the frequency response function and the Fortran part is used for the assembly of the different mass and stiffness matrices. The finite elements are 8 nodes hexaedrons anywhere in the structure. Rubber dampers are connected to the aluminium structure through their upper interface.

3. Model reduction of the dampers

Two reduction step are used in this study: the first one is a kinematical constraint that makes use of the difference of stiffness between the rubber core and the aluminium interface in the dampers. The interfaces are transformed into rigid bodies which are represented by a single point at the center of the interface, associated to three translational dofs and three rotational dofs, thus reducing any damper interface to 6 dofs only. This procedure transforms the dampers into connectors that can be attached to the structure by their upper node (reduction of the upper interface) and that can be excited through their lower node (reduction of the lower interface). The next step consists in the reduction and the condensation of the core of the dampers to their previously reduced interfaces so that only the 12 rigidified dofs stand as the finally reduced damper super element. In the following section the first reduction step is presented and then the core reduction is explained.

Table 1. Material parameters of the aluminium.

Parameters	Values
E	70 GPa
ν	0.3
ρ	2700 kg·m^{-3}

Table 2. Material parameters of the elastomer.

Parameters	Values
E	0.947 MPa
ν	0.45
ρ	1000 kg·m^{-3}
G_0	0.327 MPa
G_∞	0.126 GPa
α	0.3
τ	0.52 μs

3.1. Rigid interfaces assumption

Due to the difference between the aluminium and the elastomer stiffness, the aluminium interfaces may be considered to be rigid compared to the rubber core. A kinematical constraint is used to enforce the rigid body motion of the interfaces. The velocity of any point A of an interface can be written in terms of the velocity of the center C of the same interface and the cross-product of the distance between point A and point C and the rotation Ω of the interface. This relationship can be extended to the displacement within the context of small displacement, namely:

$$\overrightarrow{u}_A = \overrightarrow{u}_C + \overrightarrow{AC} \times \overrightarrow{\Omega} \tag{5}$$

In matrix form, the same constraint is written by:

$$\begin{bmatrix} u_A \\ v_A \\ w_A \end{bmatrix} = \begin{bmatrix} u_C + (y_C - y_A)\Omega_z - (z_C - z_A)\Omega_y \\ v_C + (z_C - z_A)\Omega_x - (x_C - x_A)\Omega_z \\ w_C + (x_C - x_A)\Omega_y - (y_C - y_A)\Omega_x \end{bmatrix} \tag{6}$$

Where x, y and z are coordinates in the 3D space, u_X, v_X and w_X are the displacements of a point X following axes $\vec{x}$, $\vec{y}$ and $\vec{z}$, and Ω_x, Ω_y and Ω_z are the interface rotation around the same axes. This relation finally leads to write any displacement of an interface point A as the product between a transfer matrix and the interface center dofs (node C):

$$\begin{bmatrix} u_A \\ v_A \\ w_A \end{bmatrix} = \begin{bmatrix} 1 & 0 & 0 & 0 & (z_A - z_C) & (y_C - y_A) \\ 0 & 1 & 0 & (z_C - z_A) & 0 & (x_A - x_C) \\ 0 & 0 & 1 & (y_A - y_C) & (x_C - x_A) & 0 \end{bmatrix} \begin{bmatrix} u_C \\ v_C \\ w_C \\ \Omega_x \\ \Omega_y \\ \Omega_z \end{bmatrix} \tag{7}$$

Following this approach, all interfaces dofs are eliminated from the global finite element model dofs list, thus reducing the computational cost of the structure model. In place of those eliminated

dofs, each damper face is now represented by 6 dofs: 3 translational dofs and 3 rotational dofs. In the next section, the reduction of the core of the dampers is done by using a Craig-Bampton sub-structuring method that consists of reducing the structure by a modal projection and then condensing the reduced system on the 12 interfaces dofs.

3.2. Model reduction of the core of the dampers

The method used here to reduce the damper finite element model combine a Craig-Bampton method [4] and a multi-model approach [2] [3]. In the case of a structure made of elastic and viscoelastic materials, the dynamic equation is given by equation (3). Following the Craig-Bampton method, boundary and internal dofs are separated. Here, the boundary nodes are the 12 dofs of the rigid interfaces noted $\mathbf{u}_\mathrm{B}$ and the internal dofs are the remaining dofs of the dampers noted $\mathbf{u}_\mathrm{I}$. This leads to write equation (3) as:

$$\left(\begin{bmatrix} \mathbf{K}^0_{\mathrm{BB}} & \mathbf{K}^0_{\mathrm{BI}} \\ \mathbf{K}^0_{\mathrm{IB}} & \mathbf{K}^0_{\mathrm{II}} \end{bmatrix} + i\omega \mathrm{h}^*(\omega) \begin{bmatrix} \mathbf{K}^\omega_{\mathrm{BB}} & \mathbf{K}^\omega_{\mathrm{BI}} \\ \mathbf{K}^\omega_{\mathrm{IB}} & \mathbf{K}^\omega_{\mathrm{II}} \end{bmatrix} - \omega^2 \begin{bmatrix} \mathbf{M}_{\mathrm{BB}} & \mathbf{M}_{\mathrm{BI}} \\ \mathbf{M}_{\mathrm{IB}} & \mathbf{M}_{\mathrm{II}} \end{bmatrix} \right) \begin{bmatrix} \mathbf{u}_\mathrm{B} \\ \mathbf{u}_\mathrm{I} \end{bmatrix} = \begin{bmatrix} \mathbf{f}_\mathrm{B} \\ \mathbf{0} \end{bmatrix} \tag{8}$$

where the right-hand side is only composed of reaction forces $\mathbf{f}_\mathrm{B}$ at the interfaces. The problem is then solved in two steps:

- The inertial terms of the preceding equation are first neglected and a static response is calculated. This response account for the behavior of the damper due to its connections with other structures at its interfaces.
- A dynamic response is then obtained by solving the eigenvalue of equation (8) with fixed boundary conditions at the interfaces. This response account for the vibrations of the damper under dynamic loading.

Solving the static problem The static response is obtained by taking $\omega = 0$ in equation (8), thus eliminating any inertial terms in the equation. Then a unit displacement is imposed on one of the boundary dof while the others are fixed. This procedure is repeated on all boundary dofs. The static internal displacements obtained are the static modes. They can be used to represent the whole response of the system when the damper is excited through its interfaces. The number of static modes is equal to the number of interfaces dofs (here 12). The static modes $\mathbf{\Psi}_{\mathrm{IB}}$ are thus obtained by solving the system:

$$\begin{bmatrix} \mathbf{K}^0_{\mathrm{BB}} & \mathbf{K}^0_{\mathrm{BI}} \\ \mathbf{K}^0_{\mathrm{IB}} & \mathbf{K}^0_{\mathrm{II}} \end{bmatrix} \begin{bmatrix} \mathbf{I}_{\mathrm{BB}} \\ \mathbf{\Psi}_{\mathrm{IB}} \end{bmatrix} = \begin{bmatrix} \mathbf{0}_{\mathrm{BB}} \\ \mathbf{0}_{\mathrm{IB}} \end{bmatrix} \tag{9}$$

where $\mathbf{I}_{\mathrm{BB}}$ is the identity matrix that stands for all unitary imposed displacements on boundary dofs. The second line of the system gives:

$$\mathbf{\Psi}_{\mathrm{IB}} = -(\mathbf{K}^0_{\mathrm{II}})^{-1} \mathbf{K}^0_{\mathrm{IB}} \tag{10}$$

This static modes are also called constrained modes. The number of static modes is equal to the number of boundary modes. Finally, the whole static response of the system can be written as the projection of the boundary displacements onto a matrix made of the identity and the constrained modes:

$$\begin{bmatrix} \mathbf{u}_\mathrm{B} \\ \mathbf{u}_\mathrm{I} \end{bmatrix} = \begin{bmatrix} \mathbf{I}_{\mathrm{BB}} \\ \mathbf{\Psi}_{\mathrm{IB}} \end{bmatrix} \mathbf{u}_\mathrm{B} \tag{11}$$

In equation (11), the internal displacement is given by $\mathbf{u}_\mathrm{I} = -(\mathbf{K}^0_{\mathrm{II}})^{-1} \mathbf{K}^0_{\mathrm{IB}} \mathbf{u}_\mathrm{B}$ where the inverse of $\mathbf{K}^0_{\mathrm{II}}$ may be seen as the flexibility of the internal dofs, while the product $\mathbf{K}^0_{\mathrm{IB}} \mathbf{u}_\mathrm{B}$ may represent a force caused by boundary displacements onto internal dofs. In fact, the constrained modes can be seen as a static correction when a linear displacement is imposed on the j^{th} boundary dof, where j is also the column number of the mode in $\mathbf{\Psi}_{\mathrm{IB}}$.

Solving the dynamic problem To get a complete solution, a static response is not enough: it has to be completed to account for the dynamic behavior of the system. By taking equation (8) in a dynamic situation, with fixed boundary conditions at the interfaces ($\mathbf{u}_\mathrm{B} = \mathbf{0}$), the following equation is obtained:

$$\left(\mathbf{K}^0_\mathrm{II} + i\omega \mathrm{h}^*(\omega)\mathbf{K}^\omega_\mathrm{II} - \omega^2\mathbf{M}_\mathrm{II}\right)\mathbf{u}_\mathrm{I} = \mathbf{0} \tag{12}$$

Solving equation (12) would lead to the vibration modes of the structure but due to the frequency dependence of the the term $i\omega\mathrm{h}^*(\omega)$, this eigenproblem is non-linear in frequency and can not be solved directly. The proposed solution is to use a multi-model approach which is inspired by the Takagi-Sugeno fuzzy model. It has been often used to represent non-linear dynamic systems by interpolating locally linear models obtained from the sampling of the non-linear system [9]. It has been applied by Balmès [3] and Rouleau [2] to build a projection basis representative of the complex non-linear eigenvalue of equation (12). The multi-model basis is here built by the combination of many smaller basis $\mathbf{\Phi}_{\omega_j}$ and each of these basis is computed by solving the pseudo-eigenvalue problem (13) where only the real part of the equation is kept:

$$\left(\mathbf{K}^0_\mathrm{II} + \Re\left(i\omega_j \mathrm{h}^*(\omega_j)\right)\mathbf{K}^\omega_\mathrm{II} - \omega_k^2\mathbf{M}_\mathrm{II}\right)\mathbf{\Phi}_{\omega_j,k} = \mathbf{0} \tag{13}$$

where ω_j values are chosen to sample the whole frequency range of interest. In any basis $\mathbf{\Phi}_{\omega_j}$ the modes are independent but the modes from two different basis may be co-linear so a Gramm-Schmidt orthonormalisation algorithm may be necessary. In the literature, two modal basis evaluated at the minimum and the maximum frequency of the range of interest combined with a static correction lead to a good approximation of the dynamic response of highly damped structures. In this study, the static correction is already taken into account by the static modes of the static response, so only the modal basis at the minimum and maximum frequency need to be computed. Solving equation (13) for $\omega = \omega_\mathrm{min}$ and $\omega = \omega_\mathrm{max}$ lead to the two basis $\mathbf{\Phi}_\mathrm{min}$ and $\mathbf{\Phi}_\mathrm{max}$ which both respect the orthogonality conditions:

$$\mathbf{\Phi}^\mathrm{T}_{\bar{\omega}}\Re\left(\mathbf{K}^*_\mathrm{II}(\bar{\omega})\right)\mathbf{\Phi}_{\bar{\omega}} = \mathrm{diag}\left(\omega_1^2, ..., \omega_\mathrm{I}^2\right) \tag{14}$$

$$\mathbf{\Phi}^\mathrm{T}_{\bar{\omega}}\mathbf{M}_\mathrm{II}\mathbf{\Phi}_{\bar{\omega}} = \mathbf{1}_\mathrm{I} \tag{15}$$

where $\bar{\omega}$ stands for ω_min or ω_max and where:

$$\mathbf{K}^*_\mathrm{II}(\bar{\omega}) = \mathbf{K}^0_\mathrm{II} + i\bar{\omega}\mathrm{h}^*(\bar{\omega})\mathbf{K}^\omega_\mathrm{II} \tag{16}$$

Both $\mathbf{\Phi}_\mathrm{min}$ and $\mathbf{\Phi}_\mathrm{max}$ diagonalize the $\Re\left(\mathbf{K}^*_\mathrm{II}(\bar{\omega})\right)$ matrix but they don't diagonalize $\mathbf{K}^0$ or $\mathbf{K}^\omega$ and this will have an impact on the further condensation step. The dynamic of the system is then reduced by truncating the basis $\mathbf{\Phi}_\mathrm{min}$ into $\mathbf{\Phi}_{\mathrm{I}p}$ and the basis $\mathbf{\Phi}_\mathrm{max}$ into $\mathbf{\Phi}_{\mathrm{I}q}$ with $p < \mathrm{I}$ and $q < \mathrm{I}$. The complete dynamic response is then obtained by combining the two truncated modal basis $\mathbf{\Phi}_{\mathrm{I}p}$ and $\mathbf{\Phi}_{\mathrm{I}q}$ into matrix $\mathbf{\Phi}_{\mathrm{I}m}$, with $m = p + q < \mathrm{I}$. A linear combination of the column of this matrix gives the dynamic response by:

$$\begin{bmatrix}\mathbf{u}_\mathrm{B}\\ \mathbf{u}_\mathrm{I}\end{bmatrix} = \begin{bmatrix}\mathbf{0}_{\mathrm{B}m}\\ \mathbf{\Phi}_{\mathrm{I}m}\end{bmatrix}\mathbf{q}_m \tag{17}$$

where $\mathbf{q}_m$ are the generalized coordinates of the dynamic response.

Building the complete response By combining the static response coming from the behavior of structures connected to the damper's interfaces, and the dynamic response from the core of the damper, a complete basis can be assembled in the form:

$$\begin{bmatrix}\mathbf{u}_\mathrm{B}\\ \mathbf{u}_\mathrm{I}\end{bmatrix} = \mathbf{R}\begin{bmatrix}\mathbf{u}_\mathrm{B}\\ \mathbf{q}_m\end{bmatrix} \tag{18}$$

The $\mathbf{R}$ matrix is a reduction matrix containing the static constrained modes $\mathbf{\Psi}_{\mathrm{IB}}$ and the vibrations modes $\mathbf{\Phi}_{\mathrm{I}m}$:

$$\mathbf{R} = \begin{bmatrix} \mathbf{I}_{\mathrm{BB}} & \mathbf{0}_{\mathrm{B}m} \\ \mathbf{\Psi}_{\mathrm{IB}} & \mathbf{\Phi}_{\mathrm{I}m} \end{bmatrix} \tag{19}$$

The projection of equation (8) onto the reduced basis $\mathbf{R}$ is:

$$\left(\begin{bmatrix} \bar{\mathbf{K}}^0_{\mathrm{BB}} & \mathbf{0}_{\mathrm{B}m} \\ \mathbf{0}_{m\mathrm{B}} & \bar{\mathbf{K}}^0_{mm} \end{bmatrix} + i\omega \mathrm{h}^*(\omega) \begin{bmatrix} \bar{\mathbf{K}}^\omega_{\mathrm{BB}} & \bar{\mathbf{K}}^\omega_{\mathrm{B}m} \\ \bar{\mathbf{K}}^\omega_{m\mathrm{B}} & \bar{\mathbf{K}}^\omega_{mm} \end{bmatrix} - \omega^2 \begin{bmatrix} \bar{\mathbf{M}}_{\mathrm{BB}} & \bar{\mathbf{M}}_{\mathrm{B}m} \\ \bar{\mathbf{M}}_{m\mathrm{B}} & \bar{\mathbf{M}}_{mm} \end{bmatrix} \right) \begin{bmatrix} \mathbf{u}_{\mathrm{B}} \\ \mathbf{q}_m \end{bmatrix} = \begin{bmatrix} \mathbf{f}_{\mathrm{B}} \\ \mathbf{0} \end{bmatrix} \tag{20}$$

where $\bar{\mathbf{K}}^\omega_{m\mathrm{B}} = \left(\bar{\mathbf{K}}^\omega_{\mathrm{B}m}\right)^{\mathrm{T}}$ and $\bar{\mathbf{M}}_{m\mathrm{B}} = \left(\bar{\mathbf{M}}_{\mathrm{B}m}\right)^{\mathrm{T}}$. The details of the different terms of these reduced matrices are given by:

$$\bar{\mathbf{K}}^0_{\mathrm{BB}} = \mathbf{K}^0_{\mathrm{BB}} + \mathbf{K}^0_{\mathrm{BI}} \mathbf{\Psi}_{\mathrm{IB}} \tag{21}$$

$$\bar{\mathbf{K}}^0_{mm} = \mathbf{\Phi}^{\mathrm{T}}_{\mathrm{I}m} \mathbf{K}^0_{\mathrm{II}} \mathbf{\Phi}_{\mathrm{I}m} \tag{22}$$

$$\bar{\mathbf{K}}^\omega_{\mathrm{BB}} = \mathbf{K}^\omega_{\mathrm{BB}} + \mathbf{K}^\omega_{\mathrm{BI}} \mathbf{\Psi}_{\mathrm{IB}} + \mathbf{\Psi}^{\mathrm{T}}_{\mathrm{IB}} \mathbf{K}^\omega_{\mathrm{IB}} + \mathbf{\Psi}^{\mathrm{T}}_{\mathrm{IB}} \mathbf{K}^\omega_{\mathrm{II}} \mathbf{\Psi}_{\mathrm{IB}} \tag{23}$$

$$\bar{\mathbf{K}}^\omega_{m\mathrm{B}} = \mathbf{\Phi}^{\mathrm{T}}_{\mathrm{I}m} \left(\mathbf{K}^\omega_{\mathrm{IB}} + \mathbf{K}^\omega_{\mathrm{II}} \mathbf{\Psi}_{\mathrm{IB}} \right) \tag{24}$$

$$\bar{\mathbf{K}}^\omega_{mm} = \mathbf{\Phi}^{\mathrm{T}}_{\mathrm{I}m} \mathbf{K}^\omega_{\mathrm{II}} \mathbf{\Phi}_{\mathrm{I}m} \tag{25}$$

$$\bar{\mathbf{M}}_{\mathrm{BB}} = \mathbf{M}_{\mathrm{BB}} + \mathbf{M}_{\mathrm{BI}} \mathbf{\Psi}_{\mathrm{IB}} + \mathbf{\Psi}^{\mathrm{T}}_{\mathrm{IB}} \mathbf{M}_{\mathrm{IB}} + \mathbf{\Psi}^{\mathrm{T}}_{\mathrm{IB}} \mathbf{M}_{\mathrm{II}} \mathbf{\Psi}_{\mathrm{IB}} \tag{26}$$

$$\bar{\mathbf{M}}_{m\mathrm{B}} = \mathbf{\Phi}^{\mathrm{T}}_{\mathrm{I}m} \left(\mathbf{M}_{\mathrm{IB}} + \mathbf{M}_{\mathrm{II}} \mathbf{\Psi}_{\mathrm{IB}} \right) \tag{27}$$

$$\bar{\mathbf{M}}_{mm} = \mathbf{\Phi}^{\mathrm{T}}_{\mathrm{I}m} \mathbf{M}_{\mathrm{II}} \mathbf{\Phi}_{\mathrm{I}m} \tag{28}$$

It is also important to note that due to the multi-model approach used in the computation of the dynamic response, a major difference arises between the method presented here and the usual Craig-Bampton: the classic method would results in null matrix in place of $\bar{\mathbf{K}}^\omega_{m\mathrm{B}}$ and the blocks $\bar{\mathbf{K}}_{mm}$ and $\bar{\mathbf{M}}_{mm}$ would be diagonals which is not the case here.

Condensing the system on it's interfaces dofs In order to further reduce the size of the system, it is proposed to condense the vibration modes unknown $\mathbf{q}_m$ on the boundary dofs. The second line of system (20) gives the following relation between the generalized coordinates $\mathbf{q}_m$ and the interfaces displacements $\mathbf{u}_{\mathrm{B}}$:

$$\mathbf{q}_m = -\left(\bar{\mathbf{K}}^0_{mm} + i\omega \mathrm{h}^*(\omega) \bar{\mathbf{K}}^\omega_{mm} - \omega^2 \bar{\mathbf{M}}_{mm} \right)^{-1} \left(\bar{\mathbf{K}}^0_{m\mathrm{B}} + i\omega \mathrm{h}^*(\omega) \bar{\mathbf{K}}^\omega_{m\mathrm{B}} - \omega^2 \bar{\mathbf{M}}_{m\mathrm{B}} \right) \mathbf{u}_B \tag{29}$$

For the undamped case, the terms in the first parentheses are diagonal so the inversion is instantaneous, but in the damped case these terms are non-diagonal and the inversion adds some computation time. In order to limit this cost, it is possible to exploit the fact that the non-diagonal matrices are sparse. Replacing equation (29) into equation (20) leads to a condensed system on the interfaces which is equivalent to a super-element where its dimension is equal to the number of interface dofs:

$$\left(\mathbf{K}_{\mathrm{super}}(\omega) - \omega^2 \mathbf{M}_{\mathrm{super}}(\omega) \right) \mathbf{u}_{\mathrm{B}} = \mathbf{f}_{\mathrm{B}} \tag{30}$$

where the super-element mass and stiffness matrices are given by:

$$\mathbf{K}_{\mathrm{super}}(\omega) = \bar{\mathbf{K}}^0_{\mathrm{BB}} + i\omega \mathrm{h}^*(\omega) \bar{\mathbf{K}}^\omega_{\mathrm{BB}} - \left(\bar{\mathbf{K}}^0_{\mathrm{B}m} + i\omega \mathrm{h}^*(\omega) \bar{\mathbf{K}}^\omega_{\mathrm{B}m} \right) \left(\bar{\mathbf{K}}^0_{mm} + i\omega \mathrm{h}^*(\omega) \bar{\mathbf{K}}^\omega_{mm} - \omega^2 \bar{\mathbf{M}}_{mm} \right)^{-1} \left(\bar{\mathbf{K}}^0_{m\mathrm{B}} + i\omega \mathrm{h}^*(\omega) \bar{\mathbf{K}}^\omega_{m\mathrm{B}} - \omega^2 \bar{\mathbf{M}}_{m\mathrm{B}} \right) \tag{31}$$

$$\mathbf{M}_{\text{super}}(\omega) = \bar{\mathbf{M}}_{\text{BB}} - \bar{\mathbf{M}}_{\text{B}m}\left(\bar{\mathbf{K}}^0_{mm} + i\omega \text{h}^*(\omega)\bar{\mathbf{K}}^\omega_{mm} - \omega^2\bar{\mathbf{M}}_{mm}\right)^{-1} \left(\bar{\mathbf{K}}^0_{m\text{B}} + i\omega \text{h}^*(\omega)\bar{\mathbf{K}}^\omega_{m\text{B}} - \omega^2\bar{\mathbf{M}}_{m\text{B}}\right) \quad (32)$$

4. Results of the study

A comparison between the reference full finite element model and the proposed super-element is made. An harmonic displacement is imposed on the structure lower interfaces, in a direction that is parallel to these interfaces: the dampers are not moving up and down but rather in a left-forward/right-backward kind of motion. The frequency range is chosen from 0 Hz to 500 Hz and the resulting displacements at observation point P (see figure (1)), for both the full reference model and the super-element, are plotted on figure (2). The displacement of point P for the full model without damping is also plotted to show that the chosen viscoelastics parameters lead to a well damped structure. In the same time, the error in displacement is plotted on figure (4). Two types of modes (damper only or full structure) are shown in figure (3) and their frequencies are plotted in vertical line on figure (2).

One hundred modes are taken in the dynamic modal basis at null frequency in the multi-model approach. The high number of modes needed here is due to the same stiffness difference that is exploited for the kinematical constraint of the dampers interfaces: the stiffness of the elastomer core is so low that around a hundred modes are found in the frequency range 0-500 Hz. The frequency limit chosen for the calculation of this modal basis is 512 Hz, which is roughly equal to the max frequency of the frequency range, so the method is accurate.

For the second basis of the multi-model, the one that contains the pseudo-normal modes at the max frequency, only ten modes are needed to give a good approximation. This is due to the fact that pseudo-normal modes are computed from the real part of the complex stiffness matrix at a given frequency. The real part of the complex modulus is greater than one thus adding stiffness to the system so a lower number of modes is present in the frequency range of interest. The frequency limit chosen for the calculation of this second modal basis is 582 Hz, which again is roughly equal to the max frequency of the frequency range.

As it can be seen on figure (2) and (4), the super-element matches the results of the reference model with a maximal error in displacement around 0.016%, thus validating the modified Craig-Bampton proposed in this work. The different computational times from both the FRF calculation of the reference model and the super-element are given in table 3. The same computer is used to do both of them. The assembly of the super-element is done once for all, before the FRF calculation, and the corresponding computational times is given under the name of Pre CPU time in table 3.

The sum of both the super-element assembly time and the FRF computational time of the modified Craig-Bampton is more than 10 times lower than the computational time of the reference model, thus further validating the present super-element approach.

Table 3. Computational time of both the reference and super-element models.

	Reference model	Super-element
Pre CPU time	-	23 min
FRF CPU time	14 h 40 min	51 min
total CPU time	14 h 40 min	1 h 14 min

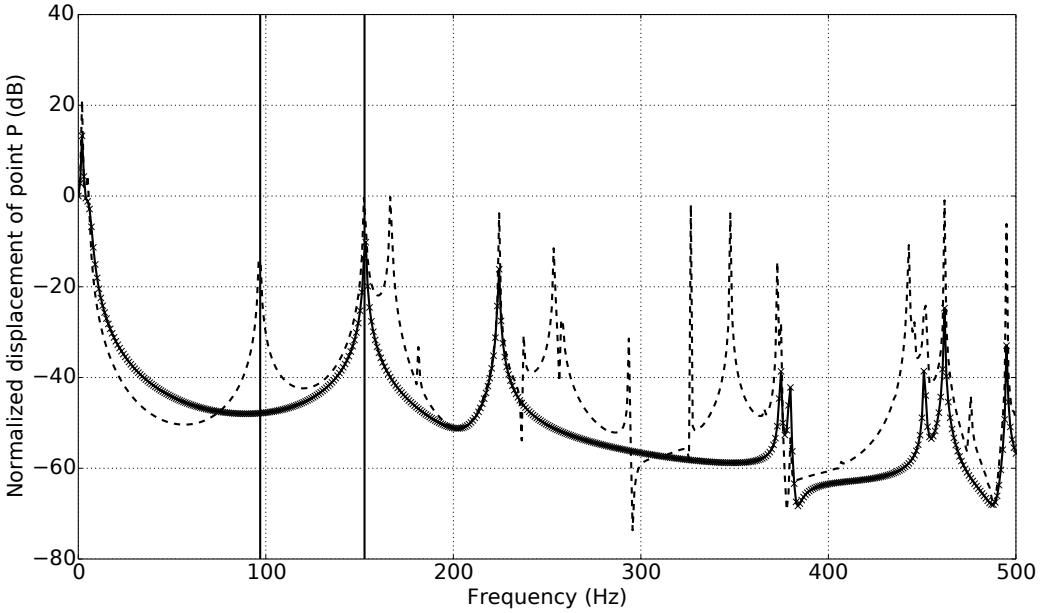

Figure 2. Normalized displacement of point P (see figure (1)) for the reference undamped model (dotted line), the reference damped (full line) and for the reduced model (cross-dotted line)

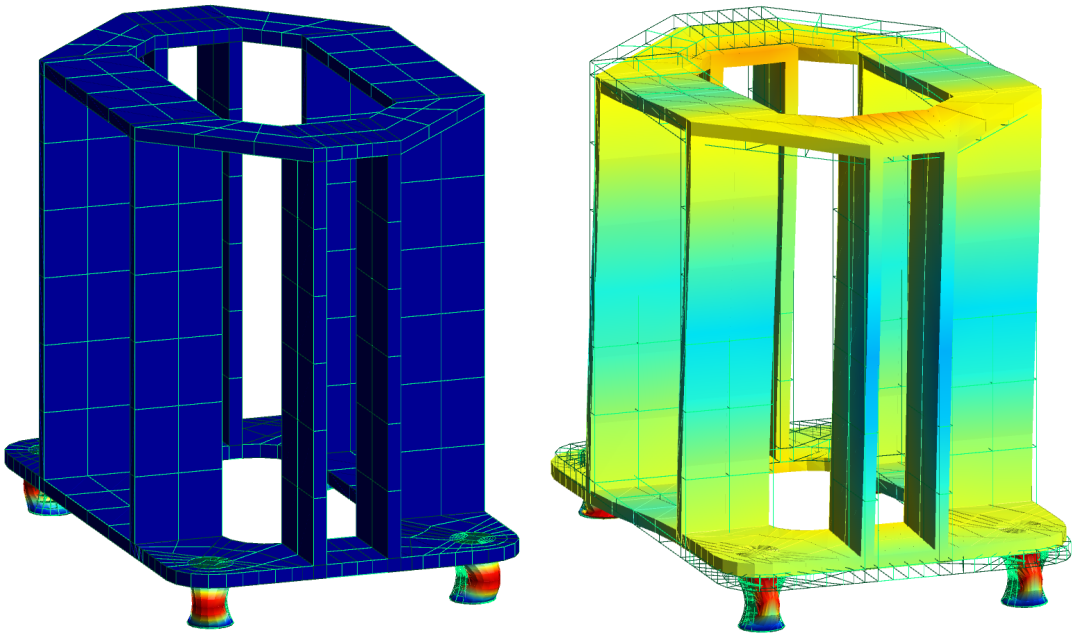

Figure 3. Modes of the undamped full structure at 98.23 Hz and 152.64 Hz (see the two vertical lines on figure 2)

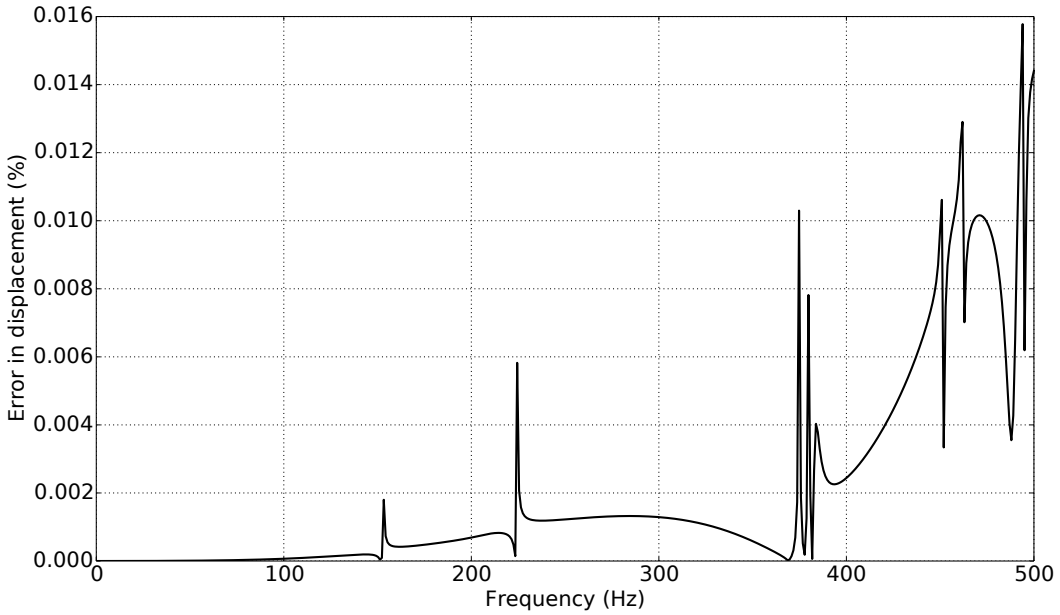

Figure 4. Error (norm 2) in displacement of the reduced model compared to the reference model

5. Conclusion

The aim of the presented method is to reduce the finite element model of a damper made of elastomer and aluminium to a 12 dofs super-element. This super-element is built through the combination of a kinematical constraint to enforce rigid body motion at the damper interface and a Craig-Bampton to reduce and condense the finite element model on it's interfaces dofs. A multi-model approach is used to keep the frequency dependence of the finite element model during the Craig-Bampton reduction process. The result is a 12 dofs super-element that replace the more than 2.10^5 dofs finite element model. This super-element can be connected to any other finite element model through its interfaces nodes, each of them having three translational dofs and three rotational dofs. To test this method, the case of an aluminium structure supported on four dampers is studied. A reference model, consisting in the structure and four non-reduced dampers, and a reduced model, made of the same structure with four super-elements, are compared. Displacements of one of the structure point are computed for both the reference and reduced models and are shown to be very close, and the error in displacement roughly stays under 0.016% on the whole frequency range thus validating the proposed method. The computational times of both models are also investigated and show that the reduced model is more than 10 times faster to compute than the reference model. A library of super-elements corresponding to different damper geometries and materials can be built off-line through this approach and then be used for design and optimization purposes in a full model.

References

[1] L. Rouleau. Modélisation vibro-acoustique de structures sandwich munies de matériaux visco-élastiques. *PhD Thesis*. Cnam, 2013.

[2] L. Rouleau, J.-F. Deü and A. Legay. Review of reduction methods based on modal projection for highly damped structures. *Proc. 11th Wor. Cong. on Comp. Mech.* 2014.

[3] A.S. Plouin and E. Balmès. Pseudo-modal representations of large models with viscoelastic behavior. *Proc. Int. Modal Analysis Conf.* 1998.

[4] R.R. Craig and M.C.C. Bampton. Coupling of substructures for dynamic analysis. *A.I.A.A.* vol 6, no 7, 1968.

[5] A.C. Galucio, J.-F. Deü and R. Ohayon. Finite element formulation of viscoelastic sandwich beams using fractional derivative operators. *Comp. Mech.* vol 33, issue 4, pp 282-291, 2004.
[6] D.M. Turner. A triboelastic model for the mechanical behavior of rubber. *Plast and Rubber, Process. and Appl.* vol 9, no 4, pp. 197-201, 1988.
[7] V.A Coveney, S. Jamil, D.E Johnson, and M.A Keavey. Implementation in finite element analysis of a triboelastic law for dynamic behaviour of filled elastomers. *Finite Element Analysis of Elastomers*. 1999.
[8] V.A Coveney, D.E Johnson, S. Jamil, and M.A Keavey. Rate dependent triboelastic and other models for elastomers and prospects for implementation in finite element analysis. *Finite Element Analysis of Elastomers*. 1999.
[9] T. Takagi and M. Sugeno. Fuzzy identification of systems and its applications to modeling and control. *IEEE Transactions on Systems, Man and Cybernetics*. No 1, pp 116-132, 1985.